Chapter

Aerosol Studies over Central India

Kannemadugu Hareef Baba Shaeb

Abstract

Earth's radiation budget and thus climate change are significantly influenced by natural and anthropogenic aerosols. Variability of aerosols both in space and time poses challenges to quantify their effects on cloud microphysical properties, precipitation and hydrological cycle. Black carbon (BC) aerosol besides having effects on human health, possess light absorbing nature and thus contribute in atmospheric radiative properties and interaction with clouds. Aerosol properties have been studied over Nagpur (79.028°E, 21.125°N) located in central India, using multi instruments such as multi wavelength radiometer, aethalometer, sunphotometer, balloon based GPS radiosonde, etc., during the study period of 2008–2014. Seasonal variability of different parameters such as aerosol optical depth, columnar water vapor, black carbon mass concentrations, mixed layer height, etc. will be discussed. MODIS aerosol and water vapor products have also been validated against ground based sunphotometer measurements. To understand the source apportionment HYSPLIT model back trajectories have been used. The chapter discusses the interesting aspect of seasonal variability of aerosol properties including monsoonal effects over the data sparse region of central India.

Keywords: aerosol, black carbon, aethalometer, radiosonde, columnar water vapor

1. Introduction

Atmospheric aerosols are solid or liquid particles suspended in air. These particles include sea salt particles, mineral dust, smoke, pollen, etc. Sources of aerosols can be from natural and anthropogenic sources. Generation of aerosols involves individual or combination of chemical, physical and biological processes. Removing processes of aerosols can be of two types, namely wet and dry deposition [1] while dominating process of aerosol removal is wet deposition (cloud and rainfall).

The environment impact assessment of these aerosols is decided by their physical and chemical properties and lifetime. The abundance, size distribution and composition of aerosol particles are highly variable both in space and time. In the lower troposphere, the total particle number concentration (typical mass concentration) typically varies in the range of about 100–100,000 cm^{-3} (1 and 100 μg m^{-3}). In the free troposphere, aerosol concentrations are (~1–2 orders) of magnitude lower than in the boundary layer.

The aerosol particles can be classified based on the size as the nucleation mode, ultrafine mode and coarse mode. Nucleation mode refers to aerosol particles below 0.1 μm in diameter, whereas diameter is lower than 0.01 μm are called ultrafine mode. The coarse mode refers to particles with diameter larger than 1.0 μm. These particles can accumulate in the atmosphere with lifetime, ranging from 1 to 7 days

(boundary layer), 3–10 days (free troposphere) and 1–365 days (in the stratosphere) and during this period they can undergo long range transport [2].

The chemical composition of atmospheric aerosol consists of variable concentrations of sulphate, nitrate, ammonium, sea salt, crustal elements and carbonaceous compounds (elemental and organic carbon) and other organic materials. Nucleation mode consists of sulphate, nitrate, ammonium, elemental and organic carbon and certain trace metals (e.g., lead, cadmium, nickel, copper, etc.). The coarse mode consists of dust, crustal elements, nitrate, sodium, chloride and biogenic organic particles (e.g., pollen, spores, plant fragments, etc.).

Atmospheric aerosol particles can absorb and scatter the incoming/outgoing shortwave and longwave radiation, which alters the radiation budget of the Earth. The also play important role in the formation of clouds and precipitation since they operate as cloud condensation and ice nuclei. Aerosols can affect significantly the cycles of nitrogen, sulphur, and atmospheric oxidants. Aerosol particles in the upper atmosphere can modify the ozone removal [3]. Additionally aerosols in the lower troposphere affect human health and mortality rate.

The effects of aerosols on climate are very uncertain. Aerosols influence the climate (forcing) in two ways, i.e., direct and indirect. In a direct effect, aerosol particles (especially sulphates) reflect incoming shortwave radiation thus cooling the Earth's atmosphere. However, this cooling effect is compensated by the absorption of longwave terreastrial radiation by absorbing aerosols (black carbon and dust particles). The annual mean radiative forcing (global) is estimated as -0.4 ± 0.2 W m^{-2} (for sulphate), -0.05 ± 0.05 W m^{-2} (for fossil fuel organic carbon), $+0.2 \pm 0.15$ W m^{-2} (for fossil fuel black carbon), $+0.03 \pm 0.12$ W m^{-2} (for biomass burning), -0.1 ± 0.1 W m^{-2} (for nitrate) and -0.1 ± 0.2 W m^{-2} (for mineral dust) [4].

Indirect effect of aerosols affect formation of cloud droplets which are formed by condensation of water vapour onto aerosol particles (cloud condensation nuclei, or ice nuclei) when the relative humidity exceeds the saturation. A very large supersaturation (about 400%) is required for the homogeneous condensation of water vapor in the absnce of aerosols. The increased number of aerosols (i.e., the increased cloud optical thickness) decreases the net surface radiation as they reflect more solar radiation (Twomey effect). Smaller particles can increase cloud lifetime. The absorption of solar radiation by absorbing aerosols can lead to evaporation of cloud particles (semi-direct effect). Anthropogenic aerosols effects on water clouds through the cloud albedo effect cause a negative radiative forcing of -0.3 to -1.8 W m^{-2} [4].

Variability of aerosol parameters over Indian region has been studied using multi-wavelength radiometer (MWR) since 1980 under the Indian Space Research Organization (ISRO) Geosphere Biosphere Program [5]. Aerosol measurements were reported from several places within the country, but such data and results are sparse in a dry tropical region in the central India.

Ground-based observations are important in order to evaluate the accuracy and validity of parameters retrieved from satellites. The validation excerise is usually targeted to the test the retrieval algorithm efficiency and how it can be improved further. India has a wide variety of ecosystems and surface conditions. Hence it is important to validate the satellite-based retrievals using ground-based measurements for different climatic regions throughout the country. Hareef Baba Shaeb et al. [6] reported the validation of the MODIS aerosol optical depth and water vapor over Nagpur located in the central Indian region. Aerosol loading at the measurement site is influenced both by local sources and long range transport. To locate the possible sources, back trajectory analysis is used. We also used MODIS detected fire locations to understand the contribution of biomass burning. They

have studied for the first time over this region focusing on the classification of aerosol types, validation of MODIS AOD and water vapor products and the role of aerosol transport. Black carbon (BC) is a primary aerosol emitted directly at the source from incomplete combustion processes such as fossil fuel and biomass burning and therefore much atmospheric BC is of anthropogenic origin (IPCC 2007). BC is receiving much attention recently owing to its effects on weather, atmospheric circulation, and hydrological cycles [7–11] and due to the adverse health impacts of BC [12, 13]. BC possess strong absorption characteristics over wide wavelength range (from UV to near IR) and its chemically inert nature (i.e., longer life time) make this species very important in global change and climate studies [14, 15].

Boundary layer dynamics play important role in surface concentrations of observed BC and its vertical dispersion (convection). The altitude up to which the surface would influence the vertical dispersion of species through convective turbulent eddies is known as the mixed layer height (MLH) and this is an important boundary layer parameter. In view of this Kompalli et al. [16] studied continuous observations of surface BC mass concentration (MBC) along with year-around vertical profiles of atmospheric thermodynamics using balloon borne GPS aided radiosonde ascents from a semi-arid suburban location Nagpur, in Central India are carried out.

The chapter discusses the interesting aspect of seasonal variability of aerosol properties over the data sparse region of central India.

2. Study location and general meteorology

Central India is surrounded by the Great Indian Desert in the northwest, Indo Gangetic Plain in the north and coastal India in east and west. The Nagpur city (21°06′N, 79°03′E; 310 m a.m.s.l) lies at the geographic center of India (**Figure 1**) on the Deccan plateau of Indian peninsula. A very dry and semi humid climate prevails throughout the year except in the monsoon season (June–September).

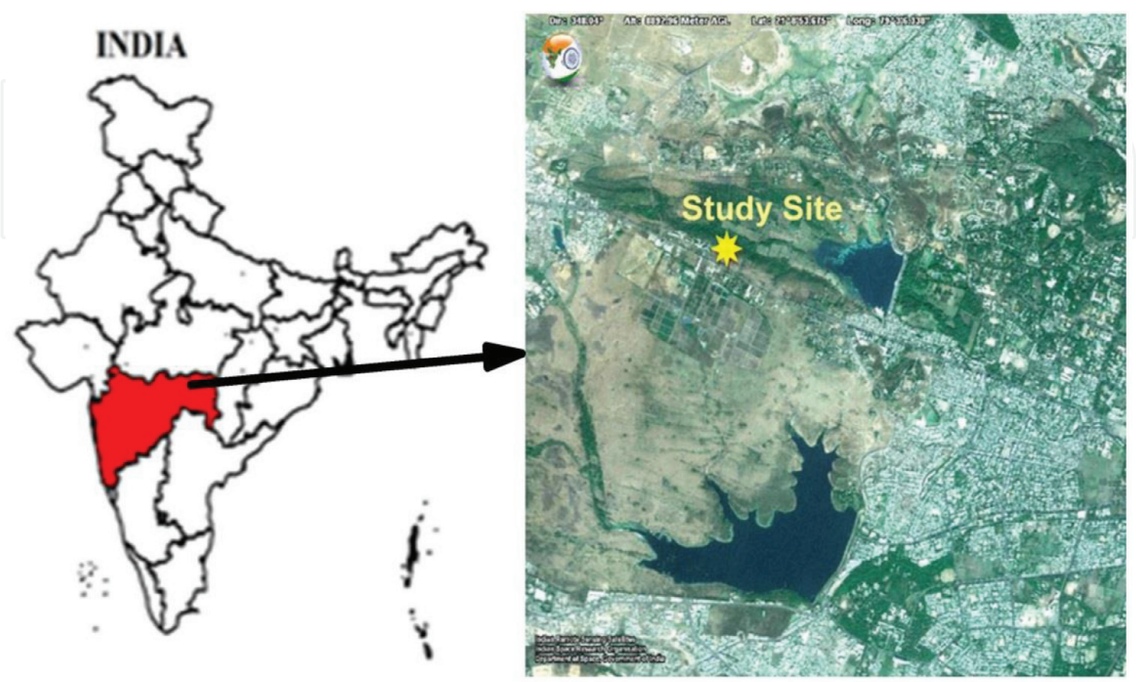

Figure 1.
Study site location.

Dry and hot weather prevails throughout the pre monsoon (PMS) season (March–May). The maximum temperature shoots up to 42–48°C. Summer monsoon (SMS) starts in June and continue up to September. Maximum rainfall is observed during July and August months. During the post monsoon (PoMS) season (October–November), the maximum temperature is about 33°C. Winter season (December, January and February) registers minimum temperatures around 12°C and at times goes below that level.

The monthly mean surface meteorological data, obtained from www.wunderground.com and rainfall data obtained from www.hydro.imd.gov.in are used for correlating measured Black carbon mass concentrations. **Figure 2(a)** shows

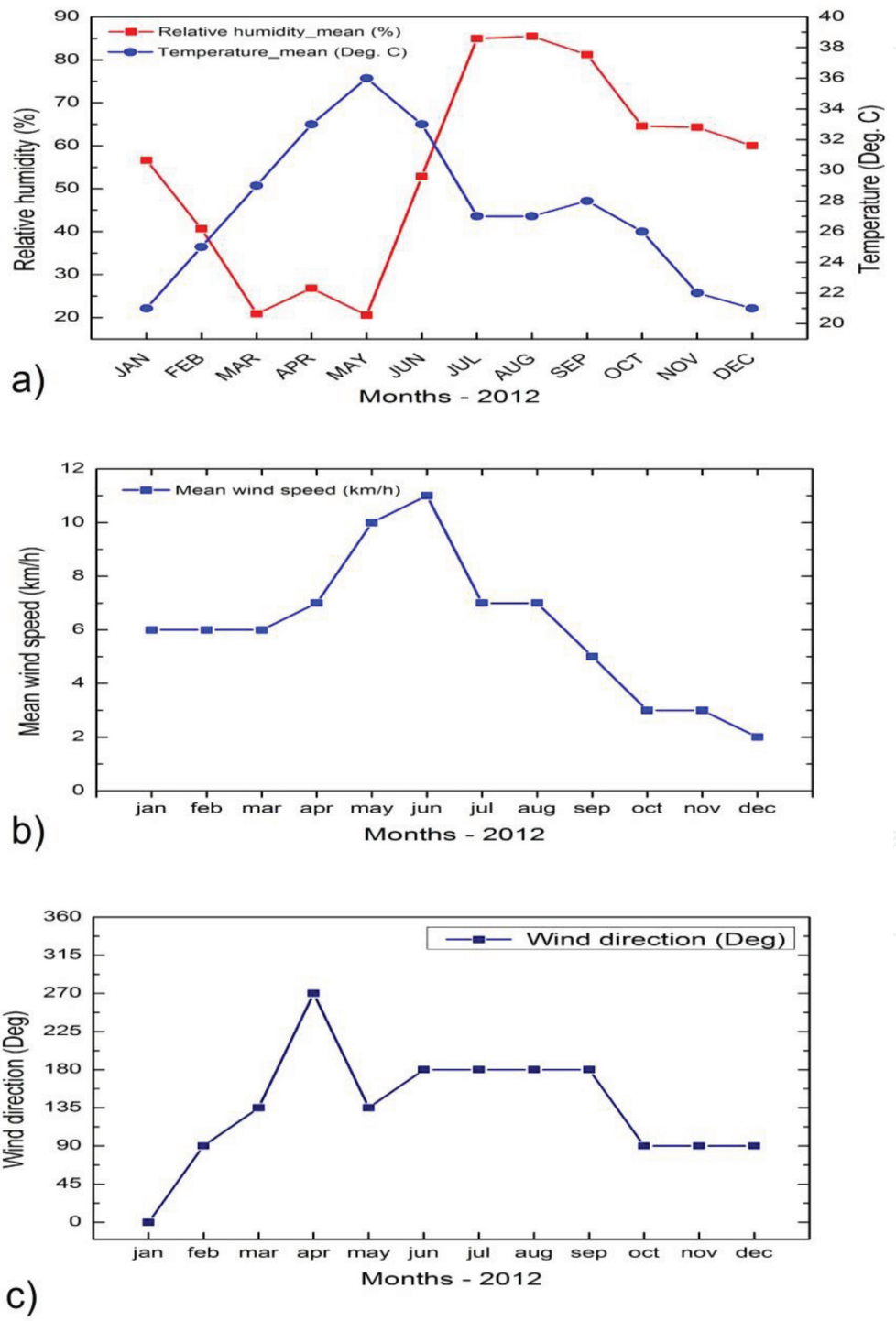

Figure 2.
Monthly variations of (a) relative humidity (%) and temperature (°C), (b) wind speed (m/s) and (c) wind direction (Deg) for 2012.

monthly means of relative humidity and temperature for the year 2012 at the site. Relative humidity is in between ~50–85% during Monsoon and ~60–80% during oost-monsoon and its highest compared to other seasons. Mean wind speed is high during monsoon season and it was observed maximum in the month of June and July. It is gradually increasing from lower values in winter months (not much variation within the winter months) to higher values in pre-monsoon and reaches maximum in monsoon months as high as (2.39 ± 0.53) m/s in the year 2012 decreases in post-monsoon months as like in the winter months. The monthly variation of mean wind speed is shown in **Figure 2(b)** for the years 2012.

Figure 2(c) shows the monthly variation of the mode of wind direction. These wind direction data is used to correlate with cluster trajectories which were used for source appointment. It was observed that mode (maximum number of times) of wind direction is constant about 3–4 months. Thus the wind direction plays a key role in the seasonal transportation of black carbon to study site.

3. Data and methods

3.1 Measurement methods

3.1.1 Ground based

3.1.1.1 Multiwavelength radiometer

Multi-Wavelength Radiometer (MWR) is a passive instrument used for studying the spectral variation in aerosol properties in the visible and near infrared region. The MWR, was mounted on the building upperside, was used to estimate spectral AOD's, on days when unobstructed solar visibility was available for 3 h or a lot of. Aerosol columnar optical depth is calcuable at 10 slender wavelength bands targeted at 380, 400, 450, 500, 600, 650, 750, 850, 935 and 1025 nm. The MWR collects the incoming solar flux as a function of solar zenith angles. The well-known Lambert–Beer–Bouguer Law (Eq. (1)) permits the estimation of AOD, because the output voltage V_λ of the MWR at any wavelength is directly proportional to I_λ, by solving a linear square fit between the logarithm of V_λ and therefore the corresponding relative air mass.

$$I\lambda = I0\lambda \exp .[-\tau_\lambda \, mr] \tag{1}$$

where $I_{0\lambda}$ = extra-atmospheric solar irradiance, m_r = relative air mass, Iλ is the direct solar irradiance at the earth's surface at wavelength λ, τ_λ = total optical thickness. The measured data was edited and further AOD values were calculable following the Langley technique [17, 18]. The total optical depth τ_λ was calculable because the the slope of the curve following the Langley plot methodology. Considering τ_λ as the total of the contribution of the various atmospheric components,

$$\tau_\lambda = \tau_{R\lambda} + \tau_{g\lambda} + \tau_{w\lambda} + \tau_{a\lambda} \tag{2}$$

$\tau_{R\lambda}$ = Rayleigh optical thickness, $\tau_{g\lambda}$ = absorption optical depth (atmospheric gases), $\tau_{w\lambda}$ = optical depth (water vapor), $\tau_{a\lambda}$ = aerosol optical depth. The calculable values of aerosol optical depth $\tau_{a\lambda}$ has errors. The error in τ_λ arises due to 1-min time resolution and the statistical errors in regression calculations. The error in Ozone (O_3) model superimposed with the seasonal differences in O_3 contributes associatean uncertainty of 10% in $\tau_{g\lambda}$ while error in $\tau_{R\lambda}$ is 0.03%. Thus $\tau_{a\lambda}$, may thus

have a most application of this methos to the MWR data analysis is described in many earlier papers [5, 19, 20].

The columnar water vapor content has been estimated from the MWR measurements at 935 and 1025 nm [21–23]. The absorption of radiation at 935 nm band is higher by more than three orders of magnitude than at 850 and 1025 nm bands. The details of application of this technique are described by Nair and Moorthy [24].

3.1.1.2 Sun photometer

Model 540 MICROTOPS-II (microprocessor-based Total Ozone Portable Spectrometer) sun photometer is a compact, portable and multi-channel sun photometer is employed to study the characteristics of columnar aerosols properties and columnar water vapor and to validate the satellite retrievals.

The physical and operational characteristics of the instrument are represented within the user's guide (http://www.solar.com/manuals.htm). The sun photometer measures solar irradiance in 5 spectral wave bands (with peak wavelengths of 440, 500, 675, 870, and 936 nm) from that it derives AOD through internal software. The filters utilized in all channels have a peak wavelength preciseness of ±1.5 nm and FWHM band pass of 10 nm (http://www.solar.com/sunphoto.html).

Derivation of AOD and water vapor employing a sun photometer has been clearly explained by Refs. [25, 26]. However; here transient outline is given.

At 440, 500, 675 and 870 nm wavelengths, AOT is derived based on the Beer–Lambert–Bouguer law as follows:

$$V_\lambda = V_{0\lambda} D - 2\exp(-\tau_\lambda M), \tag{3}$$

where, for each channel (wavelength (λ)), V_λ = the signal measured by the instrument, $V_{0\lambda}$ = the extraterrestrial signal, D = Earth-Sun distance in astronomical units, τ_λ = total optical thickness ($\tau_\lambda = \tau_{a\lambda} + \tau_{R\lambda} + \tau_{O3\lambda}$), $\tau_{a\lambda}$ = aerosol optical thickness (AOT), $\tau_{R\lambda}$ = Rayleigh (air) optical thickness, $\tau_{O3\lambda}$ = Ozone optical thickness, M = the optical air mass.

The Rayleigh ($\tau_{R\lambda}$), ozone optical thickness (τO3λ) are obtained from atmospheric models as below:

$$\tau_{R\lambda} = \mathrm{R4}\ \exp.(-\mathrm{h}/29.3/273) \tag{4}$$

$$\tau_{O3\lambda} = \mathrm{Ozabs} \times \mathrm{DOBS}/1000 \tag{5}$$

where h = altitude of the place of observation in meters,
R4 = 28773.6 × (R2 × (2 + R2) × λ − 2)2, R2 = 10–8 × {8342.13 + 2,406,030/(130 − λ − 2) + 15,997/(38.9 − λ − 2)}, λ = wavelength in μm, Ozabs = ozone absorption cross section (extracted from a lookup table based on wavelength), DOBS = ozone amount in Dobson units (extracted from a lookup table based on latitude and date of observation).

MICROTOPS II sun photometer was calibrated by its manufacturer (M/s Solar Light Control, USA) at the Mauna Loa Observatory, Hawaii which is a noise-free high-altitude site before the measurements started in 2011 at our measurement site. Aside from this, we analyzed the MICROTOPS-II output when air mass is eual to zero, which is used as calibration constant. Filter degradation, temperature effects and poor pointing towards the sun can contribute to other measurement errors. The Microtops AOT retrievals uncertainties are in the range of 0.01–0.02 [27].

AERONET stands for Aerosol RObotic NETwork formed by NASA/GSFC and is expanded by collaborators in order to cover a large spatial extent. The sun photometer measurements were performed in cloud-free conditions. For the current study, sun photometer observations are chosen from the condition that the time difference between ground based observation and MODIS flypast time is a smaller amount than quarter-hour. The data set was used because the ground truth within the validation of the Terra Moderate Resolution Imaging Spectroradiometer (MODIS) AOD_{550}.

3.1.1.3 Aethalometer

Aethalometer measures blackcarbon (absorbingaerosol) content by measuring the attenuation of a beam of light transmitted through the sample when collected on a fibrous filter (Lambert–Beer law) at 7 channels (370, 470, 520, 590, 660, 880 and 950 nm). Sixth channel (entered at 880 nm) is considered as the standard channel for BC measurements because BC is the principal absorber of light at this wavelength and other Aerosol components have negligible absorption. Aethalometer (ModelAE-42, Magee Scientific, USA) was operated daily on a 24 h cycle at a flow rate 3 L/min at sampling rate of 5 min interval and air inlet is ~12 m above the ground.

The details of principle of operation, data deduction, error budget of aethalometer, inherent uncertainties in its technique and the corrections are extensively available in the literature (e.g., [28–30]) and are not repeated. The instrumental uncertainty of the aethalometer ranges from 50% at 0.05 μg m^{-3} to 6% at 1 μg m^{-3} [30]. The inherent uncertainties in the aethalometer technique basically arise due to multiple scattering (known as C-factor) and shadowing (R-factor) effects in the filter tape [28–30].

3.1.2 Satellite data

3.1.2.1 MODIS

The MODIS flies on board the EOS Terra and Aqua satellite and measure AOD and other optical properties on a world scale daily from the year 2000 onwards. Terra and Aqua satellites are at an altitude of 705 km, cross equator at 10:30 Indian Standard Time (IST) ascending towards north and at 13:30, IST dropping towards south, respectively. MODIS has 36 bands starting from 0.4 to 14.4 μm wavelengths with three completely different spatial resolutions (250, 500 and 1000 m).

MODIS daily level-3 collection version 005 AOD data at 550 nm averaged at a 1° latitude/longitude grid to produce daily MOD08_D3.005 products from Terra satellite were used. For general climate modeling, the level 3 data provide a convenient source of data that has land and ocean measurements at a 1-degree scale combined into one file. Remer et al. [62] provided international validation of Collection 004 (C004) product over both land and ocean (compared to AERONET) and reported the expected error bars of AOD values as $\tau p\lambda = \pm 0.05 \pm 0.15\tau p\lambda$ over land, where $\tau p\lambda$ is the AOD value retrieved from the intensity measured at ground. The updated C005 algorithm rule has to be valid, to account for native biases. The aerosol properties contained among the lookup table (LUT) has to be updated for as many ground measuring sites as possible, to improve the accuracy of the retrieved AOD [31].

3.1.2.2 OMI

The Ozone Monitoring Instrument (OMI) is a space-borne spectrometer, which has global coverage on a daily basis with a spatial resolution of 13 × 24 km at nadir. This instrument measures reflected and backscattered solar radiation in UV-visible spectrum (from 250 to 500 nm). Absorbing aerosol index (AAI) or simply aerosol index (AI) is obtained from OMI (http://www.temis.nl/airpollution/absaai/absaai-omi.php?year=2012&datatype=data&freq=daily) gridded daily global level 3 data (NetCDF data format) which is available on ESA Tropospheric Emission Monitoring Internet Service (TEMIS).

The AI is expressed in the following equation:

$$\mathrm{AI} = -100 \log \left\{ \left(\frac{\mathrm{I}_{\lambda 1}}{\mathrm{I}_{\lambda 2}} \right)_{\mathrm{meas}} \right\} + 100 \log \left\{ \left[\frac{\mathrm{I}_{\lambda 1}}{\mathrm{I}_{\lambda 2}} \frac{(\mathrm{A}_{\mathrm{LER}\lambda 1})}{(\mathrm{A}_{\mathrm{LER}\lambda 2})} \right]_{\mathrm{calc}} \right\} \tag{6}$$

A_{LER} is the surface Lambert equivalent albedo which is dependent on wavelength. AI at 388 nm is obtained using λ_1 (342.5 nm) and λ_2 (388 nm) and is the residue between the measured and calculated radiance assuming Lambert equivalent reflectivity [32, 33]. Tthe presence of absorbing aerosols such as dust and smoke result in positive AI values (>0.2) and high negative values (<−0.2) represent fine non absorbing particles such as sulfates, while AAI values close to zero (±0.2) correspond to clouds or coarse mode non absorbing aerosols [34].

The magnitude of AI is influenced by parameters such as solar zenith angle, aerosol layer height, cloud reflectivity, and pressure but uncertainty/variability can be minimized through seasonal/annual averages [32]. Kascoutis et al. [32] observed that the exclusion of negative AI values may not lead to a true representation of the AI levels at a particular site.

4. Results and discussion

4.1 Seasonal variability in aerosol optical depth

Hareef Baba Shaeb et al. [6] observed that AOD values are observed to be lowest throughout the monsoon because of stronger upper winds, cloud scavenging process and rain wash out [35, 36]. Throughout the post monsoon, aerosols build up slowly and presumably undergo hygroscopic (absorptive) growth in water vapor (RH > 50%) resulting in increase in AOD. In the winter season, AOD exhibits a lot of variability, at first decreasing for the month of December and so steady increasing throughout January and February months. This will be attributed to substancial increase in CWC and temperature from December to January and February. AOD rises in its manitude from winter to summer. High temperature, in association with robust surface winds throughout summer plays a very important role in heating and lifting the top soil layer. This high convective activity and frequent prevalence of long range transport of dust from northwestern India cause increase in AOD throughout this season [37].

Figure 3 shows annual average Moderate Resolution Imaging Instrument (MODIS) Terra AOD_{550} over the Indian subcontinent and surrounding regions. AOD is found to be significant (AOD > 0.7) over northwest, IGP, North east and other parts of India shows relatively less AOD (<0.45).

High AOD_{500} (0.64 ± 0.08) is observed throughout PMS. High temperature, in association with sturdy surface winds, throughout summer plays a vital role in heating and lifting the loose soil. The incursion of wet air either from the Bay of

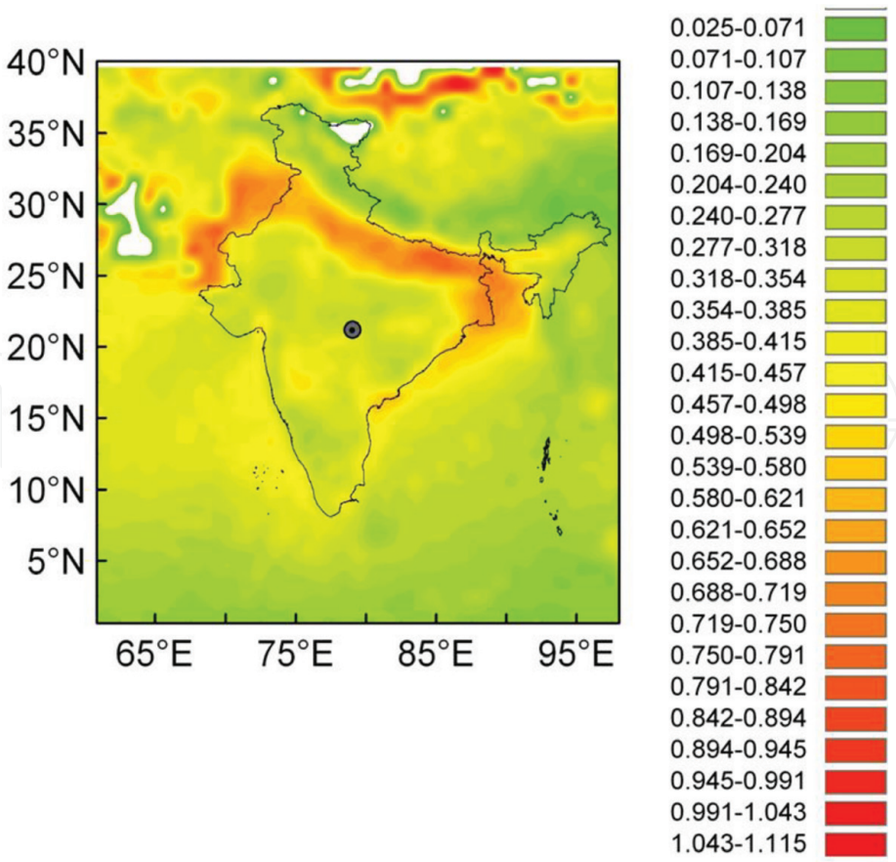

Figure 3.
Annual average moderate resolution imaging instrument (MODIS) Terra AOD_{550} over the Indian subcontinent and surrounding regions.

Bengal or Arabian Sea and/or operation of any trigger mechanism produce conditions contributing for the explosive convective development. This high convective activity and frequent incidence of long range transport of dust from northwestern result in increase in AOD throughout this season [36].

The monsoon typically advances over central India throughout the top of second week or within the third week of June and this can be characterized by severe weather activity i.e., heavy rain, thunderstorm etc. AOD_{500} values (0.38 ± 0.06) are determined to be lower throughout the monsoon season because of stronger higher winds, cloud removal and rain out processes [38]. The withdrawal of monsoon is characterized by the reversal of winds from South West to North East. During the post monsoon, aerosols build up slowly and possibly undergo hygroscopic growth in water vapor (RH > 50%) leading to increase in AOD_{500} (0.5 ± 0.02). The winter season is characterized by dry and cold weather. In the winter season, AOD_{500} is less (0.42 ± 0.15) compared to post monsoon season.

4.2 Seasonal variability in columnar water vapor

A temporal variation of columnar water vapor content (CWC) values for the period from July 2008 to June 2009 is reported by Hareef Baba Shaeb et al. [6]. Minimum columnar water vapor content value of 0.61 g/cm^2 and maximum value of 3.26 g/cm^2 is observed in the months of March 2009 and July 2008 respectively. There exists a well defined seasonal variation in CWC, with the maximum value during the monsoon months and minimum during winter months. Similar variations in columnar water vapor have been observed at other Indian locations [39–42].

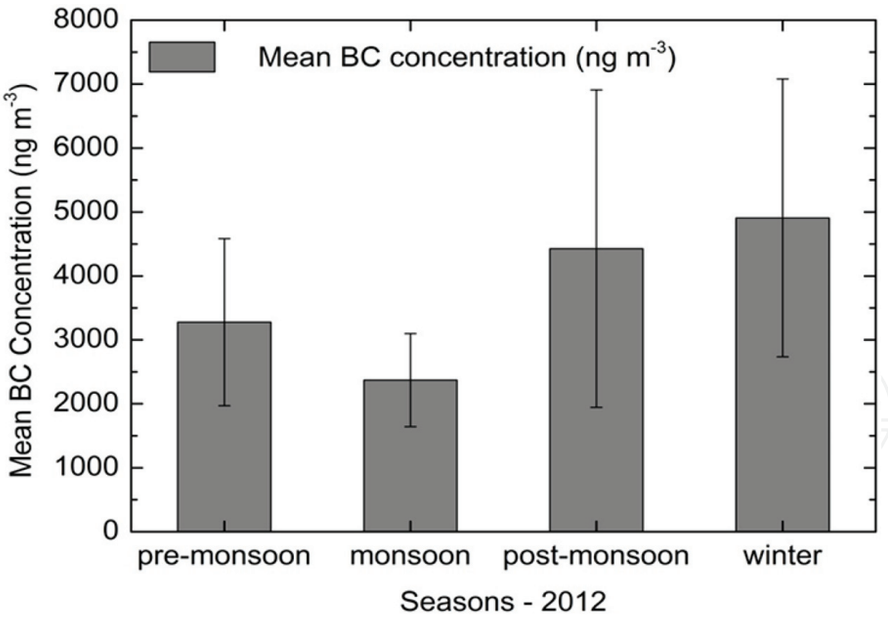

Figure 4.
Seasonal variation of black carbon concentration measured using an Aethalometer at Nagpur, during the year 2012.

It is seen that minimum CWC happens wihin the month of March and starts increasing till July and remains high throughout southwest monsoon months (June–September). CWC starts decreasing shortly once the monsoon season ends from the month of October and then a secondary minimum happens throughout the month of December.

Very good correlation $R^2 \sim 0.7$ ($R^2 \sim 0.5$) is observed between RH (%) and CWC in summer and the monsoon (post monsoon and winter). This signifies the correlation between near surface and columnar water vapor amounts.

4.3 Seasonal variations in BC mass concentration

Seasonal variations of BC aerosol mass concentration showed high values, during the post monsoon (4.4 ± 0.9 μg m^{-3}) followed by winter (4.2 ± 0.6 μg m^{-3}) season and low values during the monsoon (2.4 ± 0.6 μg m^{-3}) followed by pre monsoon (3.3 ± 0.6 μg m^{-3}) season. The variation is shown in the form of bar chart in **Figure 4**.

The annual average BC concentration is found to be 3.57 ± 0.7 μg m^{-3} and this is 20% more than the value found for the year 2011. High values of wind speed (and total rain fall) during monsoon and pre monsoon seasons may be responsible for observed low values of BC mass concentrations. During winter and post monsoon low temperatures (which keep mixed layer height low), low relative humidity leads to observed high concentrations at the surface level.

4.4 Comparisons with other locations in India

The BC mass concentrations have been compared with the measurements reported from other locations in India. This value (3.57 ± 0.7 μg m^{-3}) is lower compared to urban areas like Ahmedabad, Pune and much lower in comparison to urban and industrial locations like Delhi and Mumbai (**Table 1**).

Station	Location/ environment	Period	Mean M_{BC} (μg m^{-3})	Reference
Srinagar (34.06 °N, 74.78°E)	Northern India/urban	Jan 2013-Dec 2013	6	[43]
Darjeeling (27.03° N, 88.26°E)	Eastern India	Jan 2010 to Dec 2011	3.45	[44]
Dayalbagh, Agra (27.23°N, 78.0026° E)	Northern India (Indo-Gangetic basin)/urban	May 2014 to April 2015	9.5	[45]
Kanpur (26.46°N, 80.32°E)	Northern India (central part of IGP)/ urban	8 January 2015 to 28 February 2015	4.06 ± 2.46	[46]
Ooty (11.4°N, 76.7° E)	South India (Western ghats)/	April 2010 to May 2012	0.96 ± 0.35 (summer) 0.23 ± 0.06 (monsoon)	[47]
Ahmedabad (23.03°N, 72.55°E)	Western India/urban	Winter	11.6 ± 2.9	[48]
Mumbai (19.13°N, 72.91°E)	Western Coast/urban industrial	January to March 1999	12.5	[49]
Ananthapur (14.36°N, 77.65°E)	Southern plateau/rural (semi-arid)	August 2006 to July 2007	1.97	[50]
Hyderabad (17.47° N, 78.58°E)	South-Central India/ urban	January to July 2003	0.5–68 (dry season) 0.5–45 (wet season)	[51]
Kharagpur (22.5°N, 87.3°E)	Eastern coast of North India/industrialized	2004–2008	6.50 ± 3.04	[52]
New Delhi (28.63° N, 77.17°E)	North India/urban industrial Southern	May 2001 to April 2002	17.9 (6.7–27.9)	[53]
Trivandrum (8.5° N, 77°E)	Sothern peninsular semiurban/coastal	August 2000 to October 2001	0.3–5	[54]
Pune (18.53°N, 73.85°E)	Western/urban	January to December 2005	4.1	[55]

Table 1.
BC values reported by different authors.

4.5 Seasonal variations in mixed layer depth

In order to estimate mixed layer height (MLH), the raw data on temperature, pressure, relative humidity and geographical position (latitude, longitude and altitude) as a function of time at every 1 s, are filtered and regridded at 10 m regular interval. The top of mixed layer is defined as the altitude where the vertical gradients inθv exceeded 3 K km^{-1}. The equations used and procedure to obtain MLH is explained in Ref. [16] hence not repeated. The mean mixed layer height values for PMS, SMS, PoMS and winter are found to be 3014 ± 1187, 832 ± 452, 1871 ± 506 and 1488 ± 706 m respectively, therfore showing the least values in monsoon season, highest values in pre monsoon and moderate to low values in post monsoon and winter seasons [16].

According to Ref. [16] the main conclusion from association of MLH with BC is a good association between MLH and MBC was seen during dry period of the year (winter and PMS). However, during wet period the association between $M_{BC}$and MLH is low.

4.6 Seasonal variability in absorbing aerosol index

Annual mean variation of AAI for the year 2011 is shown in **Figure 5**. The positive values (>0.2) which represent absorbing aerosols such as dust is present in north western region (Thar desert region) and it extends even to IGP region though with less concentrations. Over Southern India the AAI values are negative indicating lesser influence of dust related aerosol particles.

Monthly mean variation of AAI at Nagpur is shown in **Figure 6**. AAI values are highly positive (>0.2) during pre-monsoon months (Mar, April, May) indicating dominance of absorbing aerosols such as dust while highly negative (<-0.2) during Monsoon (Jun, Jul, Aug, Sept) indicating the presence of non-absorbing aerosols such as sulfates. During winter (Dec, Jan, Feb) the AAI values close to zero (± 0.2) indicates the presence of clouds or coarse mode non absorbing aerosols.

4.7 Hysplit back trajectories

Hareef et al. [56] analyzed the airmass back trajectories in association with forest fires for various seasons specifically, PMS, SMS, PoMS and winter. Analysis urged that in PMS, the air masses were started from the biomass burning regions, desert

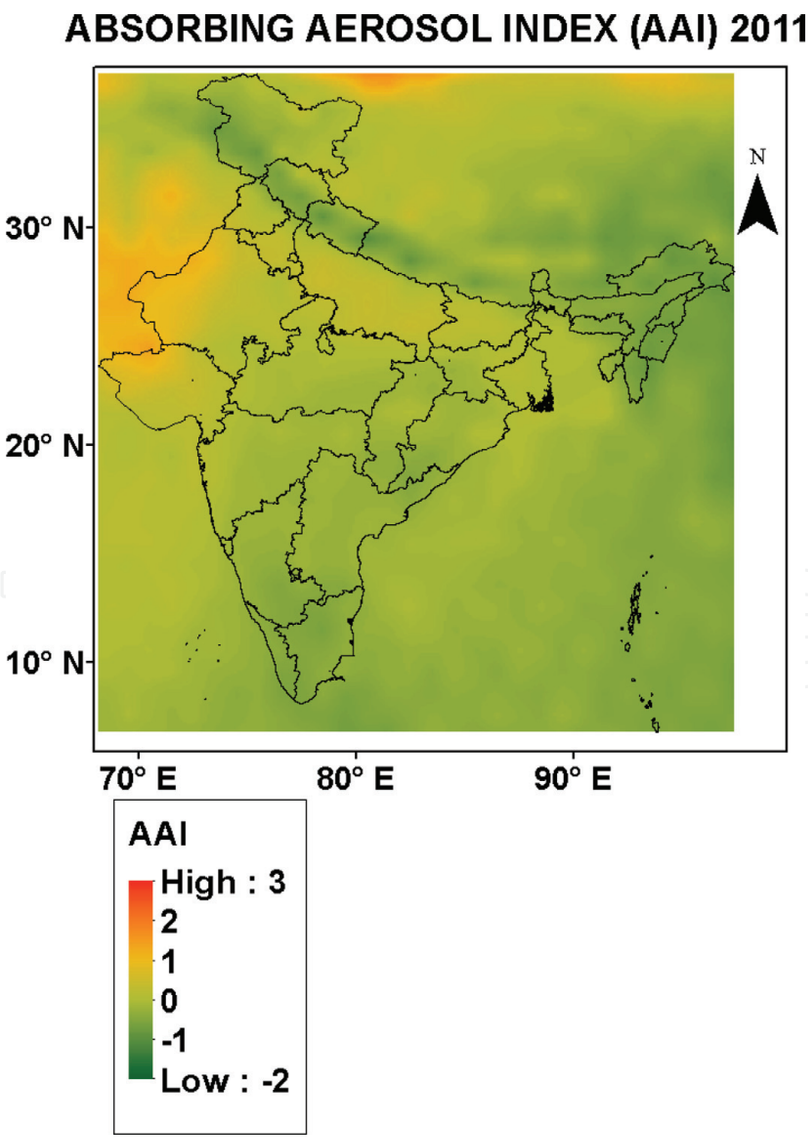

Figure 5.
Annual mean variation of AAI over India.

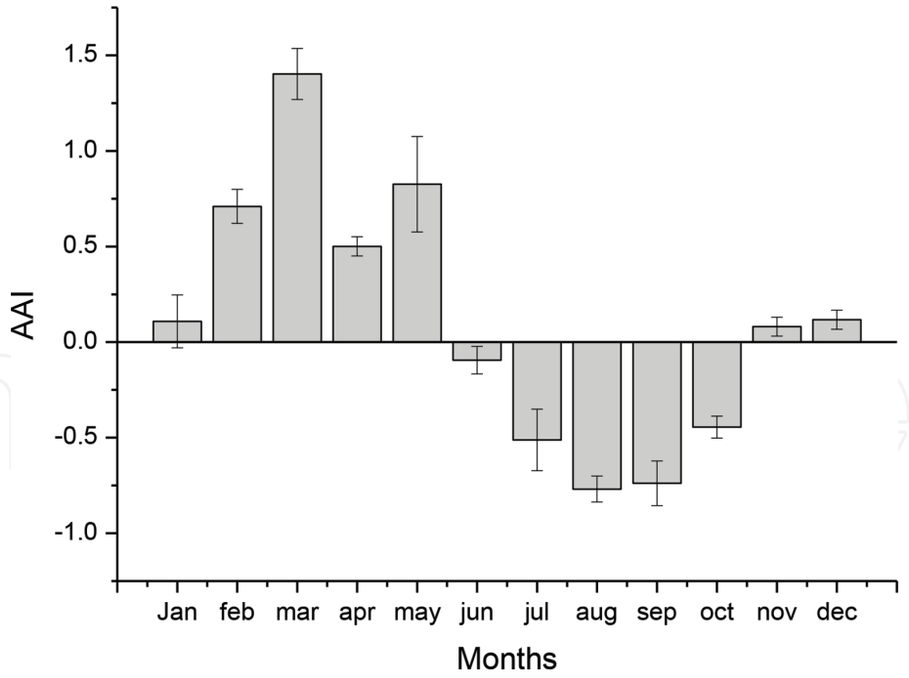

Figure 6.
Monthly variation of AAI at Nagpur.

regions and also from marine regions. During SMS, as a result of the sustained south westerly flow of the monsoon winds, the air masses were largely of marine origin. Throughout the post monsoon season, the dominant air masses were started from north India, as well as transport of air masses from biomass burning, i.e., Punjab region. Throughout winter, the origins of air masses were set in eastern India and IGP region. **Figure 7** shows example back trajectory starting at 09:00 UTC on 12 Aug 2012 at the Nagpur location.

4.8 Comparison with MODIS aerosol and water vapor products

The geophysical parameters retrieved from satellites need to be validated against the ground measurements in order to understand the retrieval errors and to correct them accordingly. This validation exercise needs to be performed for different surfaces globally. Towards this, detailed validation of MODIS AOD products of different versions with distinct spatial resolutions by using the ground-based multi wavelength radiometer and MICROTOPS sun photometer has been performed by several authors over the Indian subcontinent (e.g., [57–61]). The studies found MODIS overestimating the AOD values during the summer and underestimating during winter. Hareef et al. [56] validated the MODIS aerosol product version C005 over the central Indian region where there is no validation exercise done so far. Authors found a high correlation of 0.75 observed indicates that the MODIS can capture the seasonal variability well, and a slope of 0.65 implies an underestimation of 35% lower AOD compared to sun photometer. In the MODIS AOD retrieval algorithm, by default neutral aerosol model (Single Scattering Albedo (SSA) $\sim$ 0.9) was set for a major part of Asia [62, 63] for different seasons in a year. Absorbing (SSA $\sim$ 0.85) or non-absorbing (SSA $\sim$ 0.95) models were applied in rest of the world. This is supported by the aerosol varieties determined in AERONET sites situated at different parts around the world and supported the condition that If either the non-absorbing or the absorbing aerosol occupied more than 40% of the pie, and the other occupied less than 20%, then the location was selected as the dominant aerosol type. In India, there is just one AERONET site (IIT Kanpur: 26.28° N, 80.24°E) situated inside the IGP region and aerosol varieties determined there is

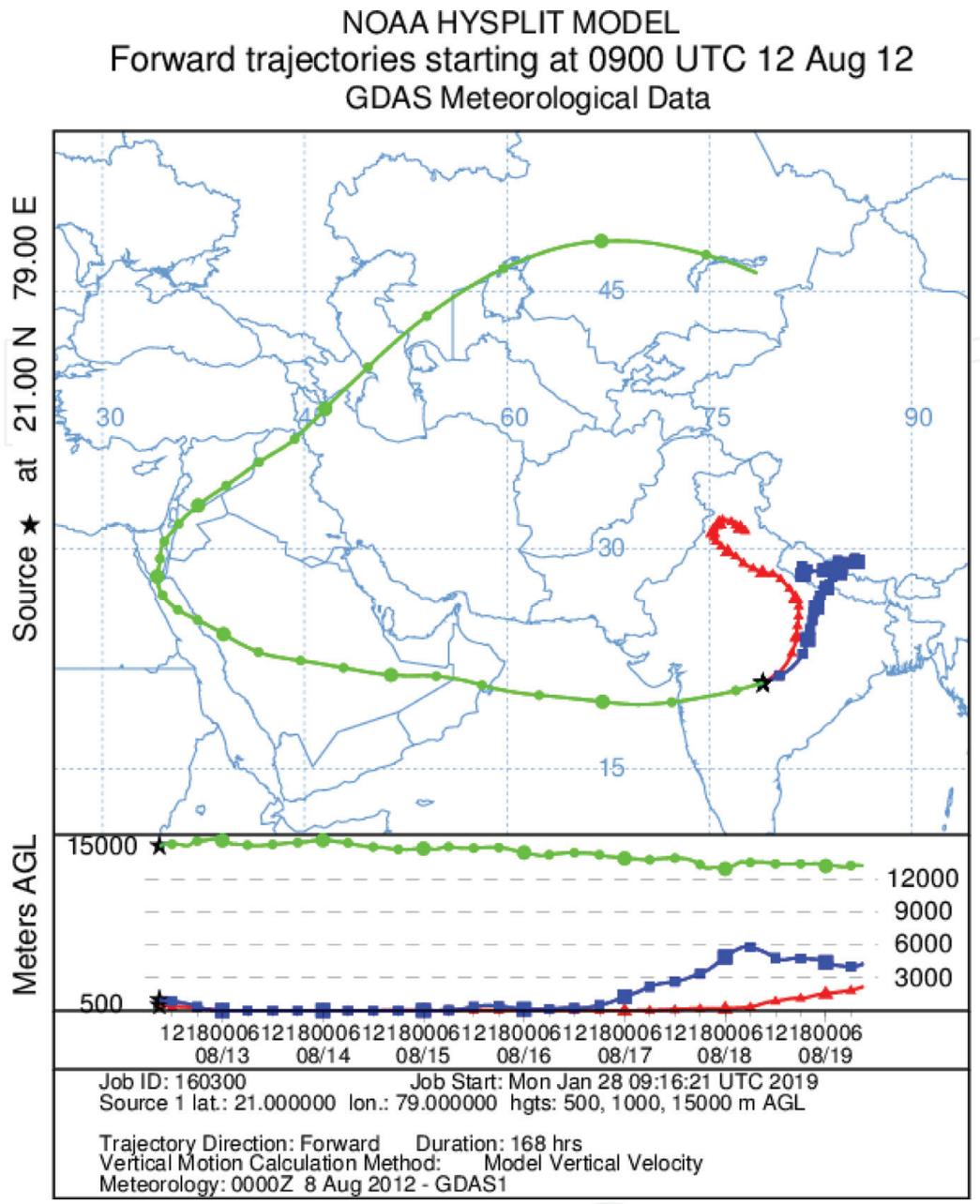

Figure 7.
Forward trajectories starting at 09:00 UTC on 12 Aug 2012 at the Nagpur location.

used in the retrieval of AOD for other locations. During PMS main aerosol types observed over Nagpur location, were UB and DD, however MODIS algorithm assumes neutral aerosol whereas there is a good proportion of UB is present that is of absorbing type. The absolute error between AOD measured (the sun photometer) to that of MODIS retrieved AOD is maximum (0.29) for this season. A decent variety of MODIS fire locations over central India and back trajectories additionally indicate that there is a transport from such places. This can cause underestimation of AOD, as for absorbing aerosols if the algorithm assumes the scattering aerosols, it will incorrectly assign a smaller AOD value to match calculated radiance with determined radiance resulting in underestimation of the AOD (retrieved from satellite). The Single Scattered Albedo for black carbon aerosols because of biomass burning is considerably not up to that of dust particles. This might be the rationale, whereas different authors reported overestimation of MODIS AOD compared to ground measured AOD, over this region, Hareef et al. [56] had observed the underestimation because of the significant amount of black carbon.

The authors concluded that the MODIS aerosol optical depth retrievals do not represent, accurately, true observations in central India, and therefore cannot be well applied there. This could be attributed to a complex nature of surface conditions and aerosol varieties and seasonal nature of surface reflectance and aerosol models over completely different ecological and geographic regions. Thus we recommend better absorbing type of model and conjointly embody seasonally dynamic changing land use/land cover options in central India for correct retrieval.

Hareef et al. [56] reported columnar water vapor (CWC) amount measured using a sun photometer over this region as typically in the 0.4–4 cm range. There exists a well-defined seasonal variation in CWC, with the maximum value during the monsoon months and minimum during winter months. Similar variations in CWC have been observed from other locations in India [5, 40]. The validation of gridded products (MODIS) is important as they are used for assimilation in numerical weather prediction and global climate models [64]. For this purpose, detailed validation of MODIS water vapor product is attempted. Validation of MODIS TERRA retrieved water vapor (NIR) with Sun photometer suggests 20% overestimation by MODIS with correlation coefficient 0.89, which has been attributed to errors due to turbidity or haze in the atmosphere.

5. Conclusions

This chapter presents the aerosol studies over Nagpur, a tropical station in central India. The main conclusions of the study are summarized as follows:

1. AOD showed highest value (0.64 ± 0.08) during the summer, while lowest during the monsoon season (0.38 ± 0.06).

2. There exists a well-defined seasonal variation in columnar water vapor content (CWC), with the maximum value during the monsoon months and minimum during winter months. Columnar water vapor (CWC) amount measured using a sun photometer over this region as typically in the 0.4–4 cm range.

3. Comparison of AOD (MODIS) and water vapor (NIR) (MODIS), with the sun photometer observations, indicates an underestimation of 35% lower AOD (correlation coefficient $\sim$0.75) and overestimation of 20% higher water vapor (correlation coefficient $\sim$0.89) respectively.

4. Aerosol transport analysis suggests during PMS, the air masses were originated from the biomass burning regions, desert regions and also from marine regions.

5. Seasonal variations of BC aerosol mass concentration showed high values, during the post monsoon (4.4 ± 0.9 μg m^{-3}) followed by winter (4.2 ± 0.6 μg m^{-3}) season and low values during the monsoon (2.4 ± 0.6 μg m^{-3}) followed by pre monsoon (3.3 ± 0.6 μg m^{-3}) season.

6. The BC mass concentrations have been compared with the measurements reported from other locations in India indicating the lower value compared to urban areas like Ahmedabad, Pune and much lower in comparison to urban and industrial locations like Delhi and Mumbai.

7. Seasonally the mean MLH values show the lowest in monsoon, highest values in PMS and moderate to low values in PoMS and winter.

8. AAI values are highly positive during pre-monsoon months, indicating dominance of absorbing aerosols such as dust while highly negative during monsoon indicating the presence of non-absorbing aerosols such as sulfates. During winter the AAI values close to zero indicates the presence of clouds or coarse mode non absorbing aerosols.

Acknowledgements

Most of the work presented in this chapter is carried out as a part of Aerosol Radiative Forcing Over India (ARFI) project of ISRO-GBP, author thanks Space Physics Laboratory for conceiving and executing such a wonderful project. Author thank Dr. Dibyendu Datta, Group Director, Climate Sciences Group, Dr. Sesha Sai M.V.R, Deputy Director, Earth and Climate Science Area and Director, NRSC for the support and encouragement towards this study. I am grateful to the NOAA Air Resources Laboratory (ARL) for the provision of the HYSPLIT transport and dispersion model through their website https://ready.arl.noaa.gov/HYSPLIT.

Conflict of interest

The author declares that there is no conflict of interest.

Author details

Kannemadugu Hareef Baba Shaeb
Earth and Climate Science Area, ISRO-Department of Space, National Remote Sensing Centre, Hyderabad, Telangana, India

*Address all correspondence to: babaphyiway@gmail.com

References

[1] Petroff A, Mailliat A, Amielh M, Anselmet F. Aerosol dry deposition on vegetative canopies. Part I: Review of present knowledge. Atmospheric Environment. 2008;**42**:3625-3653

[2] Jaenicke R. Atmospheric aerosols and global climate. Journal of Aerosol Sciences. 1980;**11**:577-588

[3] Mészáros E. Fundamentals of Atmospheric Aerosol Chemistry. Budapest: Akadémiai Kiadó; 2000. p. 308. ISBN: 9630576246

[4] Solomon S, Qin D, Manning M, Chen Z, Marquis M, Averyt KB, et al., editors. Climate Change 2007: The Physical Science Basis. Contribution of Working Group I to the Fourth Assessment Report of the Intergovernmental Panel on Climate Change. Cambridge, United Kingdom and New York, NY, USA: Cambridge University Press. p. 996. ISBN: 978 0521 88009-1

[5] Moorthy KK, Niranjan K, Narasimhamurthy B, Agashe VV, Murthy BVK. Aerosol climatology over India. In: 1-ISRO GBP MWR Network and Database, Scientific Report, ISRO GBP, SR 03. Vol. 99. India: Indian Space Research Organization; 1999

[6] Hareef Baba Shaeb K, Joshi AK, Moharil SV. Aerosol optical properties and types over Nagpur, Central India. Sustainable Environment Research. 2014;**24**(1):29-40

[7] Menon S, Hansen J, Nazarenko L, Luo Y. Climate effects of blackcarbon aerosols in China and India. Science. 2002;**297**:2250-2253. DOI: 10.1126/science.1075159

[8] Lau KM, Kim MK, Kim KM. Asian summer monsoon anomalies induced by aerosol direct forcing: The role of the Tibetan Plateau. Climate Dynamics. 2006;**26**:855-864. DOI: 10.1007/s00382-006-0114-z

[9] Meehl GA, Arblaster JM, Collins WD. Effects of black carbon aerosols on the Indian monsoon. Journal of Climate. 2008;**21**:2869-2882

[10] Gautam R, Hsu NC, Lau KM, Kafatos M. Aerosol and rainfall variability over the Indian monsoon region: Distributions, trends and coupling. Annales de Geophysique. 2009;**27**:3691-3703

[11] Lawrence MG, Lelieveld J. Atmospheric pollutant outflow from southern Asia: A review. Atmospheric Chemistry and Physics. 2010;**10**:11017-11096. DOI: 10.5194/acp-10-11017-2010

[12] Janssen NA, Hoek G, Simic-Lawson M, Fischer P, van Bree L, ten Brink H, et al. Black carbon as an additional indicator of the adverse health effects of airborne particles compared with PM10 and PM 2.5. Environmental Health Perspectives. 2011;**119**:1691-1699. DOI: 10.1289/ehp.1003369

[13] Janssen NAH, Gerlofs-Nijland ME, Lanki T, Salonen RO, Cassee F, Hoek G, et al. Health Effects of Black Carbon. Denmark: World Health Organization; 2012. ISBN: 978 92 890 0265 3

[14] Bond TC, Doherty SJ, Fahey DW, Forster PM, Berntsen T, DeAngelo BJ, et al. Bounding the role of black carbon in the climate system: A scientific assessment. Journal of Geophysical Research. 2013;**118**. DOI: 10.1002/jgrd.50171

[15] Zha S, Cheng T, Tao J, Zhang R, Chen J, Zhang Y, et al. Characteristics and relevant remote sources of black carbon aerosol in Shanghai. Atmospheric Research. 2014;**135–136**: 159-171

[16] Kompalli SK, Suresh Babu S, Krishna Moorthy K, Manoj MR, Kiran Kumar NVP, Hareef Baba Shaeb K, et al. Aerosol black carbon characteristics over Central India: Temporal variation and its dependence on mixed layer height. Atmospheric Research. 2014; **147-148**(523):27-37

[17] Shaw GE, Regan JA, Herman BM. Investigations of atmospheric extinctions using direct solar radiation measurements made with a multiple wavelength radiometer. Journal of Applied Meteorology. 1973:12374-12380

[18] Moorthy KK, Nair PR, Krishna Murthy BV. Multi wavelength solar radiometer network and features of aerosol spectral optical depth at Trivandrum. Indian Journal of Radio and Space Physics. 1989;**18**:194-120

[19] Moorthy KK, Saha A, Prasad BSN, Niranjan K, Jhurry D, Pillai PS. Aerosol optical depths over peninsular India and adjoining oceans during the INDOEX campaigns: Spatial, temporal and spectral characteristics. Journal of Geophysical Research. 2001;**106**: 28539-28554

[20] Saha A, Moorthy KK. Impact of precipitation on aerosol spectral optical depth and retrieved size distributions: A case study. Journal of Applied Meteorology. 2004;**43**(6):902-914

[21] Leckner B. The spectral distribution of solar radiation at the earth's surface—Elements of a model. Solar Energy. 1978: 20143-20150

[22] Kneizys FX, Shettle EP, Gallery WO, Chetwynd JH Jr, Abreu LW, Selby JEA, et al. Atmospheric Transmittance/ Radiance: Computer Code, Lowtran 5. AFGL-TR-80-0067. MA, USA: AFGL; 1980

[23] Tanaka M, Nakazawa T, Fukabori M. Absorption of the ρστ, 0.8 um and α bands of the water vapour. Journal of Quantitative Spectroscopy and Radiative Transfer. 1982;**28**:463-470

[24] Nair PR, Moorthy KK. Effects of changes in the atmospheric water vapour content on the physical properties of atmospheric aerosols at a coastal station. Journal of Atmospheric and Solar Terrestrial Physics. 1998;**60**: 563-572

[25] Ichoku C, Levy R, Kaufman YJ, Remer LA, Li RR, Martins VJ, et al. Analysis of the performance characteristics of the five-channel microtops II sun photometer for measuring aerosol optical thickness and precipitable water vapor. Journal of Geophysical Research. 2001;**106**: 14573-14582

[26] Morys M, Mims FM III, Hagerup S, Anderson SE, Baker A, Kia J, et al. Design, calibration, and performance of microtops II handheld ozone monitor and sun photometer. Journal of Geophysical Research. 2001;**106**: 14573-14582

[27] Holben BN, Tanre D, Smirnov A, Eck TF, Slutsker I, Abuhassan N, et al. An emerging ground-based aerosol climatology: Aerosol optical depth from AERONET. Journal of Geophysical Research. 2001;**106**:12067-12097

[28] Weingartner E, Saathoff H, Schnaiter M, Streit N, Bitnar B, Baltensperger U. Absorption of light by soot particles: Determination of the absorption coefficient by means of aethalometers. Journal of Aerosol Science. 2003;**34**:1445-1463

[29] Arnott WP, Hamasha K, Moosmuller H, Sheridan PJ, Ogren JA. Towards aerosol light-absorption measurements with a 7-wavelength aethalometer: Evaluation with a photoacoustic instrument and 3-wavelength nephelometer. Aerospace Science and Technology. 2005;**39**(1): 17-29

[30] Corrigan CE, Ramanathan V, Schauer JJ. Impact of monsoon transition on the physical and optical properties of aerosols. Journal of Geophysical Research. 2006;**111**: D18208

[31] Levy RC, Remer LA, Kleidman RG, Mattoo S, Ichoku C, Kahn R, et al. Global evaluation of the collection 5 MODIS dark-target aerosol products over land. Atmospheric Chemistry and Physics. 2010;**10**:10399-10420

[32] Kaskaoutis DG, Nastos PT, Kosmopoulos PG, Kambezidis HD. The combined use of satellite data, air-mass trajectories and model applications for monitoring of the dust transport over Athens Greece. International Journal of Remote Sensing. 2010;**31**:5089-5109. DOI: 10.1080/01431160903283868.

[33] Herman JR, Bhartia PK, Torres O, Hsu C, Seftor C, Celarier E. Global distribution of UV-absorbing aerosols from Nimbus 7/TOMS data. Journal of Geophysical Research. 1997;**102**: 16911-16922

[34] Torres O, Tanskanen A, Veihelmann B, Ahn C, Braak R, Bhartia PK, et al. Aerosols and surface UV products from ozone monitoring instrument observations: An overview. Journal of Geophysical Research. 2007; **112**:D24S47. DOI: 10.1029/ 2007JD008809

[35] Kaskaoutis DG, Badarinath KVS, Kharol SK, Sharma AR, Kambezidis HD. Variations in the aerosol optical properties and types over the tropical urban site of Hyderabad, India. Journal of Geophysical Research. 2009;**114**: D22204. DOI: 10.1029/2009JD012423

[36] Flossman FI, Hall WD, Pruppacher HR. A theoretical study of the wet removal of atmospheric pollutants—Part I: The redistribution of aerosol particles captured through nucleation and impaction scavenging by growing cloud drops. Journal of the Atmospheric Sciences. 1985;**42**:583-606

[37] Badarinath KVS, Kharol SK, Kaskaoutis DG, Kambezidis HD. Dust storm over Indian region and its impact on the ground reaching solar radiation case study using multi-satellite data and ground measurements. Science of the Total Environment. 2007;**384**: 316-332

[38] Balakrishnaiah G, Raghavendra Kumar K, Suresh Kumar Reddy B, Rama Gopal K, Reddy RR, Reddy LSS, et al. Analysis of optical properties of atmospheric aerosols inferred from spectral AODs and Angstrom wavelength exponent. Atmospheric Environment. 2011;**45**:1275-1285

[39] Ernest Raj P, Devara PCS, Saha SK, Sonbawne SM, Dani KK, Pandithurai G. Temporal variations in sun photometer measured precipitable water in near IR band and its comparison with model estimates at a tropical Indian station. Atmosfera. 2008;**21**(4):317-333

[40] Ranjan RR, Ganguly ND, Joshi HP, Iyer KN. Study of aerosol optical depth and precipitable water vapour content at Rajkot, a tropical semi arid station. Indian Journal of Radio and Space Physics. 2007;**36**:27-32

[41] IMAP FINAL REPORT-III. Characteristics of Aerosol Spectral Optical Depths over India, ISRO-IMP-SR-43-94. 1994. pp. 1-78

[42] Bhat MA, Romshoo SA, Beig G. Aerosol black carbon at an urban site-Srinagar, Northwestern Himalaya, India: Seasonality, sources, meteorology and radiative forcing. Atmospheric Environment. 2017;**165**:336-348

[43] Sarkar C, Chatterjee A, Singh AK, Ghosh SK, Raha S. Characterization of black carbon aerosols over Darjeeling—A high altitude Himalayan station in Eastern India. Aerosol and Air Quality

Research. 2015;**15**:465-478. DOI: 10.4209/aaqr.2014.02.0028

[44] Gupta P, Singh SP, Jangid A, Kumar R. Characterization of black carbon in the ambient air of Agra, India: Seasonal variation and meteorological influence. Advances in Atmospheric Sciences. 2017;**34**(9):1082-1094. Available from: https://link.springer.com/article/10.1007/s00376-017-6234-z

[45] Navaneeth M, Thamban SNT, Moosakutty SP, Kuntamukkala P, Kanawade VP. Internally mixed black carbon in the Indo-Gangetic Plain and its effect on absorption enhancement. Atmospheric Research. 2017;**197**: 211-223. Available from: http://home.iitk.ac.in/~snt/pdf/Thamban_AR_2017.pdf

[46] Udayasoorian C, Jayabalakrishnan RM, Suguna AR, Gogoi MM, Suresh Babu S. Aerosol black carbon characteristics over a high-altitude Western Ghats location in Southern India. Annales de Geophysique. 2014;**32**: 1361-1371. DOI: 10.5194/angeo-32-1361-2014

[47] Ramachandran S, Kedia S. Black carbon aerosols over an urban region: Radiative forcing and climate impact. Journal of Geophysical Research. 2010; **115**:D10202. DOI: 10.1029/2009JD013560. Available from: https://agupubs.onlinelibrary.wiley.com/doi/pdf/10.1029/2009JD013560

[48] Venkatraman C, Habib G, Eiguren-Fernandez A, Mignel AH, Friedlander SK. Residential biofuels in South Asia: Carbonaceous aerosol emissions and climate impacts. Science. 2005;**307**: 1454-1456

[49] Kumar KR, Narasimhulu K, Balakrishnaiah G, Reddy BSK, Gopal KR, Reddy RR, et al. Characterization of aerosol black carbon over a tropical semi-arid region of Anantapur, India. Atmospheric Research. 2011;**12–27** (530):100

[50] Latha KM, Badarinath KVS. Black carbon aerosols over tropical urban environment—A case study. Atmospheric Research. 2003;**69**:125-133

[51] Rai K, Sarkar AK, Mitra AP. Chemical characterization of aerosols. IASTA Bulletin. Delhi: NPL; 2002;**14**: 155-158

[52] Kompalli SK, Moorthy KK, Babu SS. Rapid response of atmospheric BC to anthropogenic sources: Observational evidence. Atmospheric Science Letters. 2013;**15**(3):166-171. DOI: 10.1002/asl2.483. Published online in wileyonline library.com

[53] Rai K, Sarkar AK, Mitra AP. Chemical characterization of aerosols at NPL, Delhi. Proceedings of a conference on aerosol remote sensing in global change and atmospheric pollution. IASTA Bulletin. 2002, 1982;**14/1**(special issue):155-158

[54] Babu SS, Moorthy KK. Aerosol black carbon over a tropical coastal station in India. Geophysical Research Letters. 2002;**29**(23):131e-1341e

[55] Safai PD, Kewat S, Praveen PS, Rao PSP, Momin GA, Ali K, et al. Seasonal variation of black carbon aerosols over a tropical urban city of Pune, India. Atmospheric Environment. 2007; **41**(13):2699-2709

[56] Hareef Baba Shaeb K, Varghese AO, Mukkara SR, Joshi AK, Moharil SV. Aerosol type's classification and validation of MODIS aerosol and water vapor products using a sun photometer over central India. Aerosol and Air Quality Research (AAQR). 2015;**15**(2): 682-693

[57] Tripathi SN, Dey S, Chandel A, Srivastava S, Singh RP, Holben BN. Comparison of MODIS and AERONET

derived aerosol optical depth over the Ganga Basin, India. Annales de Geophysique. 2005;**23**:1093-1101

[58] Prasad AK, Singh S, Chauhan SS, Srivastava MK, Singh RP, Singh R. Aerosol radiative forcing over the Indo-Gangetic Plains during major dust storms. Atmospheric Environment. 2007;**41**:6289-6301

[59] Misra A, Jayaraman A, Ganguly D. Validation of MODIS derived aerosol optical depth over Western India. Journal of Geophysical Research. 2008; **113**:D04203

[60] Vinoj V, Satheesh SK, Moorthy KK. Aerosol characteristics at a remote Island: Minicoy in Southern Arabian Sea. Journal of Earth System Science. 2008;**117**:389-397

[61] Guleria RP, Kuniyal JC, Rawat PS, Thakur HK, Sharma M, Sharma NL, et al. Validation of MODIS retrieval aerosol optical depth and an investigation of aerosol transport over Mohal in North Western Indian Himalaya. International Journal of Remote Sensing. 2012;**33**:5379-5401

[62] Remer L, Kaufman YJ, Tanre D, Mattoo S, Chu DA, Martins J, et al. The MODIS aerosol algorithm, products, and validation. Journal of the Atmospheric Sciences. 2005;**62**:947-973

[63] Levy RC, Remer LA, Dubovik O. Global aerosol optical properties and application to moderate resolution imaging spectroradiometer aerosol retrieval over land. Journal of Geophysical Research. 2007;**112**:1-15

[64] Prasad AK, Singh RP. Validation of MODIS Terra, AIRS, NCEP/DOE AMIP-II reanalysis-2, and AERONET Sun photometer derived integrated precipitable water vapor using ground-based GPS receivers over India. Journal of Geophysical Research. 2009;**114**: D05107